JOURNAL OF APPLIED POLYMER SCIENCE VOL. 20, 3087–3103 (1976)

The Thermal Transition Behavior of Polyorganophosphazenes*

N. S. SCHNEIDER, C. R. DESPER, and R. E. SINGLER, *Organic Materials Laboratory, U.S. Army Materials and Mechanics Research Center, Watertown, Massachusetts 02172*

Synopsis

The thermal transition behavior of poly[bis(trifluoroethoxyphosphazene)] (I) and two samples of poly[bis(*p*-chlorophenoxyphosphazene)] (II) have been studied as representative alkoxy- and aryloxy-substituted polyorganophosphazenes. Several of the polymers of this class are reported to exhibit two first-order transitions, denoted herein as $T(1)$ for the transition from a crystalline to mesomorphic state and T_m for the true melt. Studies of these two polymers were undertaken to gain a further understanding of this behavior. Optical microscopy on a solution-cast film of I showed that the details of spherulitic morphology persist through $T(1) = 90°C$ and remain undisturbed through the temperature interval up to $T_m = 240°C$. The study of II by x-ray diffraction reveals that two sharp lines are observed above $T(1) = 165°C$ and that orientation is not randomized upon heating to temperatures as high as 238°C. Considerable improvement in the crystalline diffraction pattern results from the thermal treatment. A detailed examination was also made by differential scanning calorimetry (DSC) of the effects of cycling through $T(1)$, annealing in the temperature interval between $T(1)$ and T_m and for I, the influence of controlled crystallization from the melt. The results indicate that the organization in the mesomorphic state, as influenced by thermal history, has a profound affect on the peak position, area, and sharpness of the endotherm at $T(1)$. For I, the apparent heat of fusion at $T(1)$ is about ten times greater than at T_m, whereas for II, no DSC peak is observed at $T_m = 365°C$, suggesting that the ratio of the heats of fusion at $T(1)$ and T_m is greater than 50. However, estimated volume changes at the two transitions are nearly equal. These results are compared with those of other polymers which exhibit an intermediate state of order and with molecular liquid crystals.

INTRODUCTION

A variety of semicrystalline polyphosphazene homopolymers has now been prepared by the procedure first outlined by Allcock,[1] and some of the properties of these polymers have been summarized in two recent reviews.[2,3] The first detailed characterization of crystalline polyphosphazenes was carried out by Allen[4] who discovered that several of the polymers displayed two widely separated first-order transitions. An x-ray examination of an alkoxy substituted sample, poly[bis(trifluoroethoxy)phosphazene], showed that the lower transition at 90°C, herein designated $T(1)$, corresponded to a transformation from a crystalline to mesomorphic state. Above $T(1)$, the pattern was reduced to a single sharp reflection at 11 Å which was interpreted as representing lateral chain packing order. Optical microscopy showed that birefringence persisted up to

* Based on presentation given at the Polyphosphazene Conference, AMMRC, Watertown, Massachusetts, May 1975.

© 1976 by John Wiley & Sons, Inc.

the true melting temperature T_m = 240°C, confirming the existence of a partially ordered state above $T(1)$. The dynamic mechanical data reported by Allen[4] and Gillham[5] reveal that a major drop in modulus occurs above $T(1)$. The polymer in this semifluid state between $T(1)$ and T_m can be compression molded to a coherent film. More recent data dealing particularly with aryloxy polyphosphazenes[3] have shown that two first-order transitions separated by as much as 250°C are found in samples with a wide variety of substituent structure.

The purpose of the present work is to examine in detail the phase transition behavior in a representative alkoxy and aryloxy polyphosphazene sample, as part of a continuing investigation of the properties of this class of polymers.

EXPERIMENTAL

The samples used in this study were prepared by the bulk ring-opening polymerization of hexachlorocyclotriphosphazene, followed by the conversion of the resulting poly(dichlorophosphazene) to the polyorganophosphazene. This procedure has been described in detail elsewhere.[3] The poly[bis(trifluoroethoxy)phosphazene] (I) was prepared in this laboratory. Two samples of poly[bis(*p*-chlorophenoxy)phosphazene] (II) were used in this study. Sample IIa was prepared in this laboratory while sample IIb was received from Horizons Inc., Cleveland, Ohio:[6]

I II

A summary of the synthesis conditions and sample analyses is provided in Table I. The samples were compression molded about 10° above their respective $T(1)$ transitions at 100 bars to obtain films approximately 10 mil thick which were used in the physical characterization studies. X-Ray diffraction patterns were recorded with a Warhus camera equipped with heated sample holder using copper K_α radiation and a sample-to-film distance of 31.40 mm. The differential scanning calorimetry (DSC) studies were carried out under nitrogen using the Perkin-Elmer DSC II, while penetrometer and thermal expansion measurements were conducted under helium with the Perkin-Elmer TMS I system. In addition, optical microscopy was performed on samples cast from tetrahydrofuran at room temperature directly onto microscope slides. A Nikon microscope equipped with polarizer and analyzer and a Reichart heating stage were used for examining the films.

TABLE I
Synthesis of Polyorganophosphazenes

Sample	Polymerization *t*/*T*	Yield, %	Substitution *t*/*T*	Yield,[a] %	Elemental analysis, % actual (calculated) C	H	N	Cl
I	72 hr/240°C	40	1 hr/50°C	60	19.7	1.55	5.62	0.039
			5 hr/23°C		(19.8)	(1.66)	(5.76)	(0)
IIa	16 hr/260°C	58	16 hr/110°C	79	48.2	2.78	4.78	23.6
IIb	18 hr/250°C	—	22 hr/125°C	71	48.0	2.90	—	23.6
	10 hr/270°C				(48.0)	(2.69)	(4.76)	(23.6)

[a] Based on poly(dichlorophosphazene). For I, $[\eta]$ = (0.66 dl/g) IIa, $[\eta]$ = 3.0 dl/g; IIb, $[\eta]$ = 1.64 dl/g.

RESULTS

Observations by Optical Microscopy and X-Ray Diffraction

The large-scale spherulitic structure typical of a solution-cast film (see experimental) of the poly[bis(trifluoroethoxy)phosphazene] is shown in Figure 1. The detailed morphology remains unaltered on heating through $T(1) = 90°C$, although an increase in transmission indicated that a change in birefringence

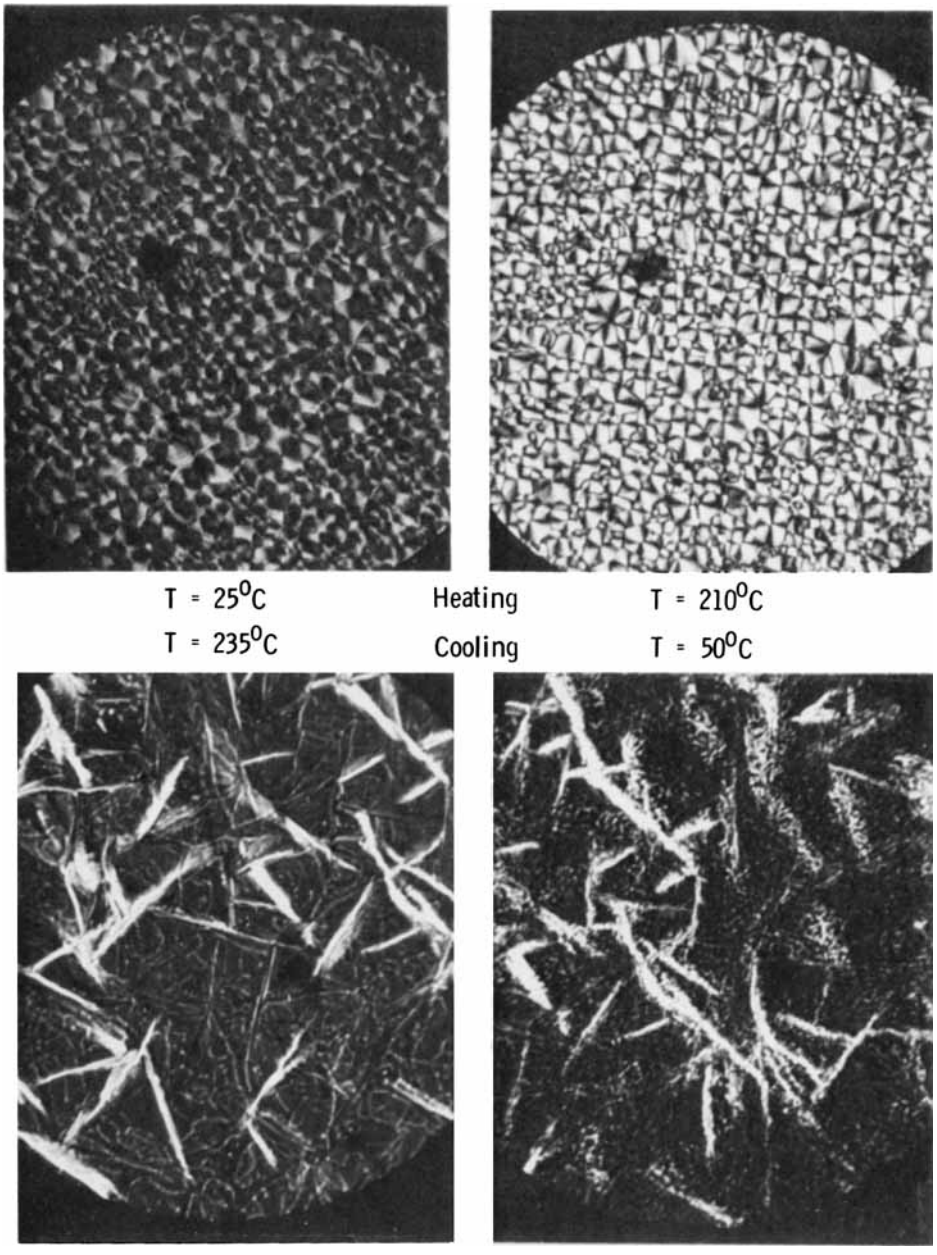

Fig. 1. Optical micrographs, film of polymer I solution cast from tetrahydrofuran at room temperature, 100× magnification.

has occurred. The behavior is reversible if the temperature remains below the melting temperature T_m = 240°C. Recrystallization after heating above T_m produces needle-shaped crystals rather than the original spherulitic morphology. With poly[bis(*p*- chlorophenoxy)phosphazene], similarly prepared samples resulted in films with an indistinct texture which was below the resolving power of the optical microscope, and the true melting temperature was beyond the range of the heating stage.

The x-ray diffraction pattern of I was generally similar at $T(1)$ to that reported by Allen.[4] However, a pronounced improvement in the crystalline diffraction pattern could be obtained by heating the sample in the DSC above $T(1)$ and particularly by heating above T_m to 250°C followed by controlled cooling at 10°/min. Similar behavior in sample IIb is illustrated by the x-ray diffraction patterns obtained on the heating and cooling cycles as shown in Figures 2a and 2b and summarized in Table II. Annealing at 146°C results in a marked improvement in the structure. At 199°C, which is about 30°C above $T(1)$, two sharp reflections are observed indicating that structure is still present. The

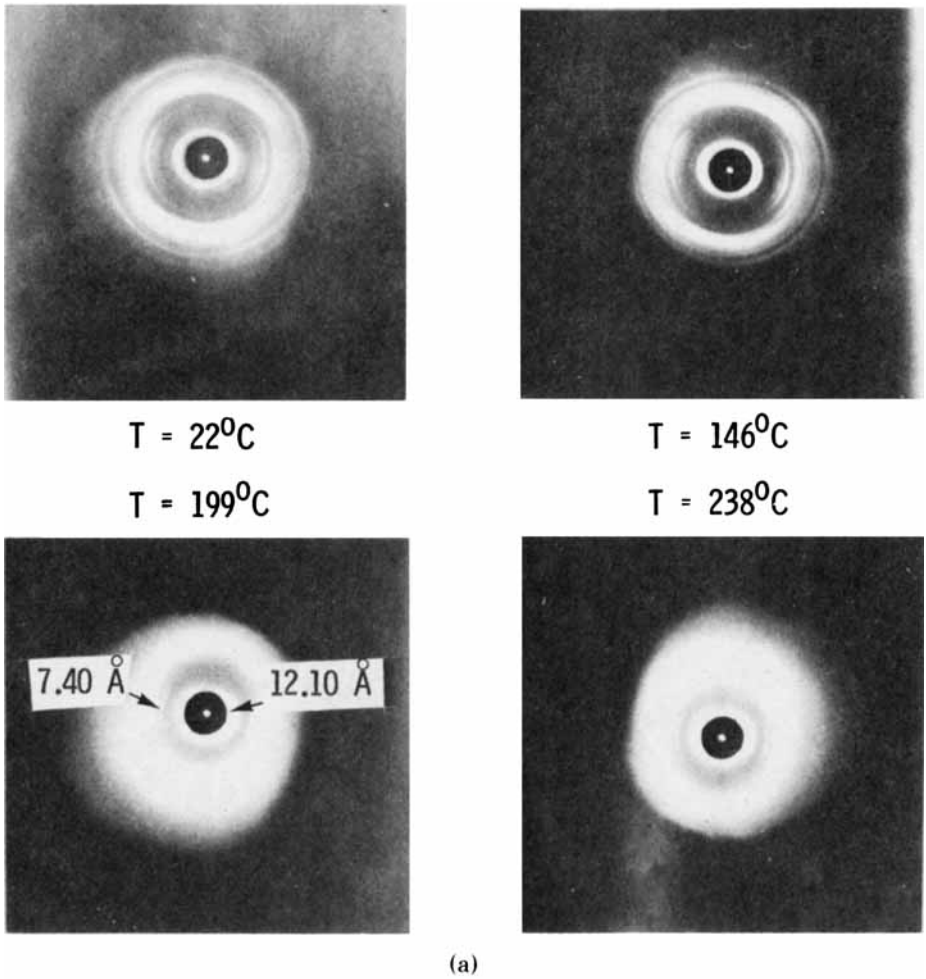

(a)

Fig. 2 (*continued*)

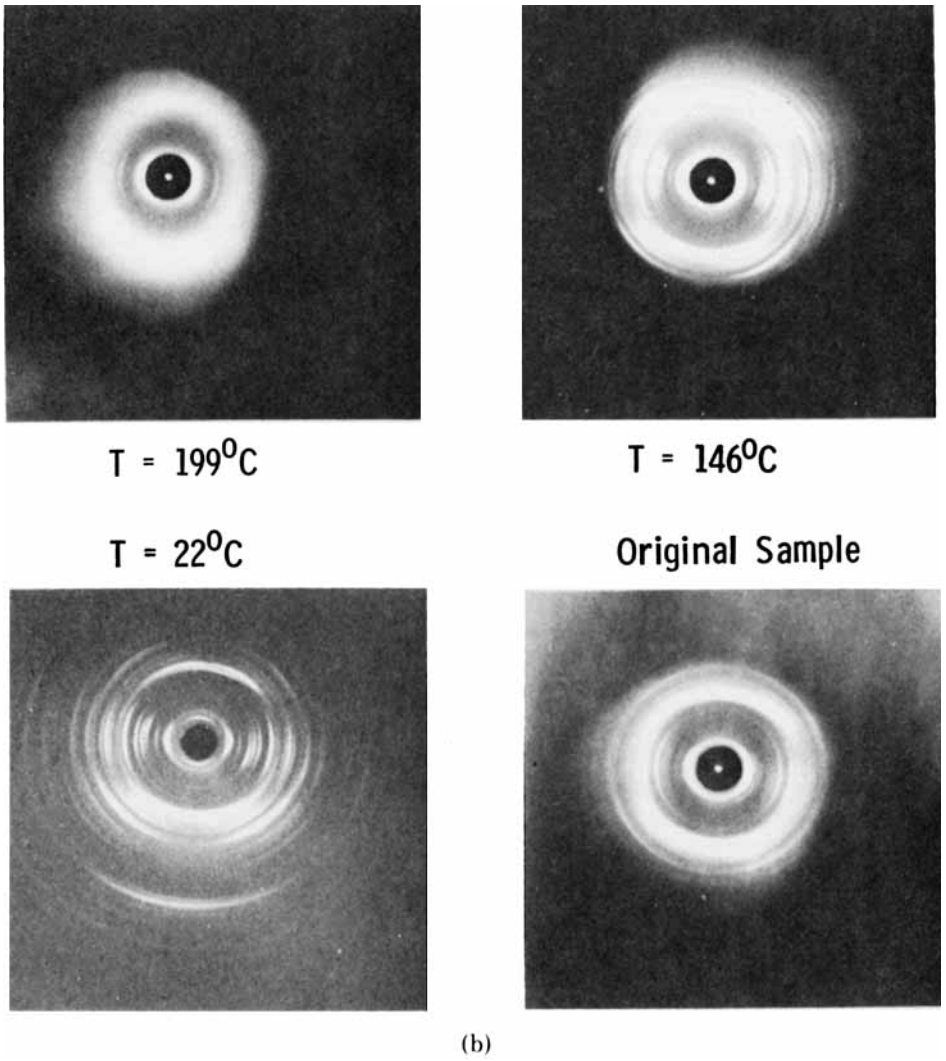

Fig. 2. X-Ray diffraction pattern, compression molded film of IIb: (a) heating cycle, maximum temperature 238°C; (b) cooling cycle.

positions of these lines are indicated by the arrows in Figure 2a for the 199°C pattern. Whereas the reflection at 7.40 Å shows clearly, the intense equatorial reflection at 12.10 Å is located within the broad inner halo and is not evident in the print. It is noteworthy that the partial orientation resulting from compression molding of the sample is not randomized throughout the above heating cycle. The pattern which results on cooling after the prolonged thermal cycle shows a marked improvement in order compared to the original. The absence of any distinct amorphous halo suggests that the polymer is now highly crystalline. Anomalous lines appearing at 13.61 and 4.68 Å (Table II) correspond to lines observed with hexakis(*p*-chlorophenoxy)cyclotriphosphazene (trimer). Liquid chromatography indicates the presence of about 6% oligomeric species, including trimer, in the sample as prepared and this amount is probably increased

TABLE II
X-Ray Diffraction of Poly[bis(*p*-chlorophenoxy)phosphazene] (IIb)

Temperature, °C	Observed orthorhombic lines		Anomalous sharp lines	Broad line
	HK	HKL		
22	3	3	None	none
146	4	5	None	none
199	none	none	12.10,7.40 Å	4.4 Å
238	none	none	12.18,7.12 Å	4.4 Å
199	none	none	11.74,7.12 Å	4.3 Å
146	15	6	11.66,6.59,4.35 Å	none
22	14	15	13.61,6.45,4.68 Å	none

TABLE III
Comparison of Thermal Transition Data

Sample	$T(1)$, °C	T_m, °C	$\Delta H(T(1))$, cal/g	$\Delta H(T_m)$, cal/g	$\Delta V(T(1))$, %	$\Delta V(T_m)$, %
Poly[bis(trifluoroethoxy)phosphazene]	92	240	8.6	0.8	5	6
Poly[bis(*p*-chlorophenoxy)phosphazene]	169	356	6.6	0	3.5	5.7
Polyethylene		141		68		15
p-Azoxyanisole	116	133	28	0.7	0.1	0.36

by the prolonged thermal cycle. Otherwise, the pattern can be indexed in terms of the orthorhombic unit cell proposed by Bishop and Hall,[7] but the 6.45 Å line corresponding to the 200 reflection appears unusually intense compared to their result.

DSC Analysis

The thermal transitions determined by DSC, penetrometer, and thermal expansion methods are summarized in Table III. Our principal concern is with the nature of the transitions at $T(1)$ and T_m and the response of the transformation temperature for the crystalline to mesomorphic transition to repeated thermal cycling or annealing procedures. For convenience, $T(1)$ will be referred to as a melting temperature. Where confusion might arise, the transition to the liquid state will be designated as the true melting temperature. We will discuss first the behavior of the poly[bis(trifluoroethoxy)phosphazene], denoted as I, and then the two different preparations of poly[bis(*p*-chlorophenoxy)phosphazene], designated IIa and IIb.

The appearance of the endotherm at $T(1)$ for I in a series of melting and crystallization cycles is depicted in Figure 3. The first melt of the compression-molded sample produces a broad endotherm with a peak at 79.5°C which corresponds to the transition temperature previously reported.[4] After cooling and recrystallization from 385°K at 20°/min, the melting endotherm on the second cycle has sharpened appreciably and the area has increased by about 10%. If the sample is repeatedly scanned between 320° and 385°K, the peak position continues to advance by 1° or so, and the area under the endotherm increases by about 6% in each cycle. Changes of this magnitude occur in each successive

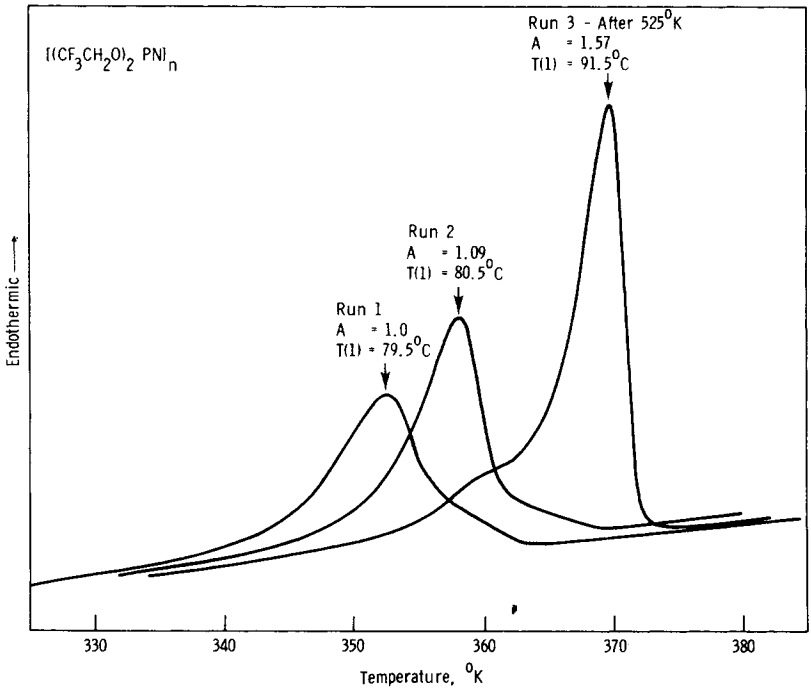

Fig. 3. Influence of thermal cycling on the crystalline-to-mesomorphic transition in I: heating rate, 10°/min; cooling rate, 20°/min; attentuation, 5 mcal/sec; heating cycles, 300° to 385°K. Run 3 obtained after heating through T_m to 255°C.

cycle for at least four or five cycles. Alternatively, it is possible to induce a marked change in T_m by annealing briefly at temperatures between $T(1)$ and T_m. For example, after 5 min at 200°C, a value of $T(1) = 86$°C is obtained. No endotherm is shown in Figure 3 for the sample at this stage. Until now, the sample has only been cycled below T_m. When the sample is recrystallized after heating through T_m to $T = 255$°C, there is a dramatic increase in the area and sharpness of the melt endotherm, and the peak temperature has now moved to 91.5°C as illustrated in Figure 3.

The effect of repeated cycling through $T(1)$ after recrystallization from above T_m is shown in Figure 4. The first scan displays the enhanced endotherm which results by cooling from the true melt. In the second run, the endotherm has broadened and moved to the lower temperature. An additional cycle results in a further reduction in the transition temperature. That this is not due to degradation or to irreversible changes in the sample is shown by reheating through T_m and recrystallization which restores the initial features to the endotherm. This observation indicates that heating through $T(1)$ disorders the structure of the mesomorphic state which has been produced by slow cooling from the true melt. Possibly, this is a result of the significant volume change which occurs at $T(1)$ as discussed below. The strong influence of thermal prehistory above $T(1)$ on the crystalline x-ray diffraction pattern and the behavior of the endotherm at $T(1)$ suggest that the organization of the mesomorphic state is subject to modification and that this, in turn, can influence the nature of the crystalline structure formed at lower temperatures.

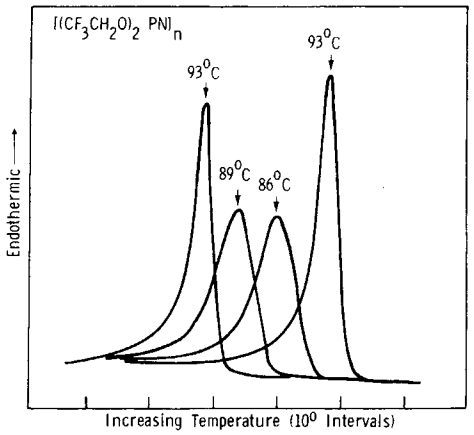

Fig. 4. Effect of cycling following recrystallization from the melt for sample I. From left to right: runs 1, 2, and 4, 320° to 385°K; run 3, 320° to 525°K. Heating, 10°/min; cooling rate, 20°/min; attenuation, 5 mcal/sec. Successive curves displaced by arbitrary amounts along the temperature axis.

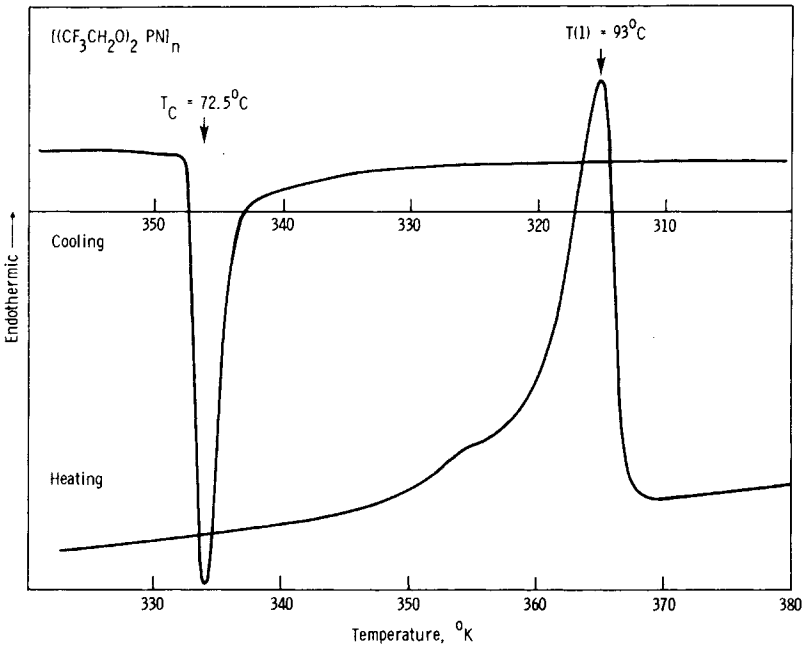

Fig. 5. Melting endotherm and crystallization endotherm at $T(1)$ for sample I: heating cycle, 300° to 385°K, 10°/min; attenuation, 5 mcal/sec; cooling cycle, 385° to 300°K, 10°/min; attenuation, 10 mcal/sec.

The appearance of the recrystallization exotherm for sample I is illustrated in Figure 5. The onset of crystallization is sharply defined and occurs at a supercooling of about 20°C as indicated by the temperature interval between the melting and recrystallization peaks. It should be noted that crystallization continues over a considerable temperature range below the exothermic peak, indicating the presence of species which are more difficult to crystallize. These

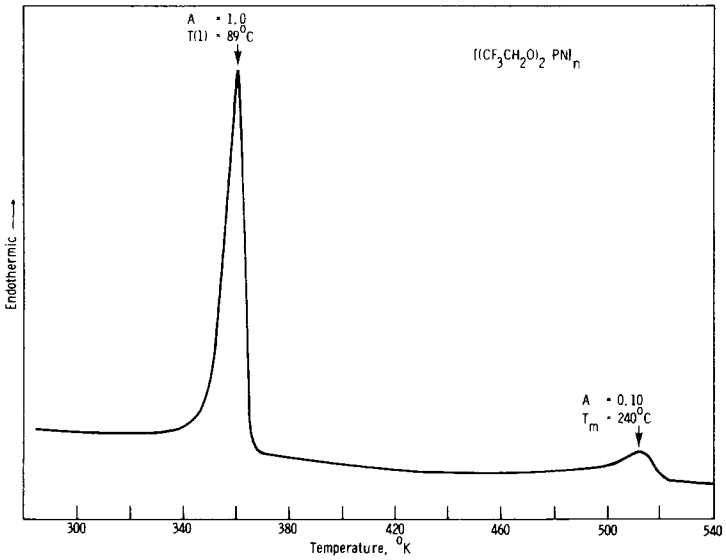

Fig. 6. Comparison of the endotherms at $T(1)$ and T_m for sample I after recrystallization from the melt: heating rates, 10°/min; attenuation, 5 mcal/sec.

same species probably contribute to the low melting fraction of the sample which comprises the leading edge of the melting peak. Further evidence for the presence of inhomogeneity in the chain structure will be pointed out in a discussion of the behavior of sample II.

A comparison of the endotherm at $T(1)$ and at T_m is shown in Figure 6. The enthalpy change at $T(1)$ is tenfold greater than at T_m (see Table II for apparent heats of fusion), and the peak is appreciably sharper than the true melt peak. Some additional features of the behavior at T_m are shown in Figure 7 taken from scans with a 20-fold increase in sensitivity over that in the previous figure. The rather broad character of the melting endotherm is clearly illustrated in the first run. Annealing carried out at 509°K, somewhat into the melting peak, succeeds in producing a higher melting component on the second run. Since this has no effect on the characteristics of the $T(1)$ transition, annealing effects were not examined further. The crystallization from the melt, shown in Figure 7, occurs at a supercooling comparable to the mesomorphic-to-crystal transformation, but the exotherm is broader than that observed for the mesomorphic-to-crystal transformation.

The melting behavior of sample IIa at $T(1)$ on the first melt and in later recrystallization and melting cycles is depicted in Figure 8. The initial melt of the compression-molded sample (run 1) produces a broad but simple endotherm. With repeated cycling between 360° and 450°K, the endotherm moves upward in temperature, increases in area, and separates into two peaks. After five cycles, most of the lower-melting portion of the sample has been transformed into the higher melting form which has a transition temperature of 165.3°C (run 5). Annealing for 2 min at 525°K eliminates the low-melting shoulder with little change in the $T(1)$ transition, as indicated by the final endotherm in Figure 8. Further annealing at 525°K, or a brief exposure to 580°K, is capable of further increasing the area beyond that shown without affecting the peak temperature.

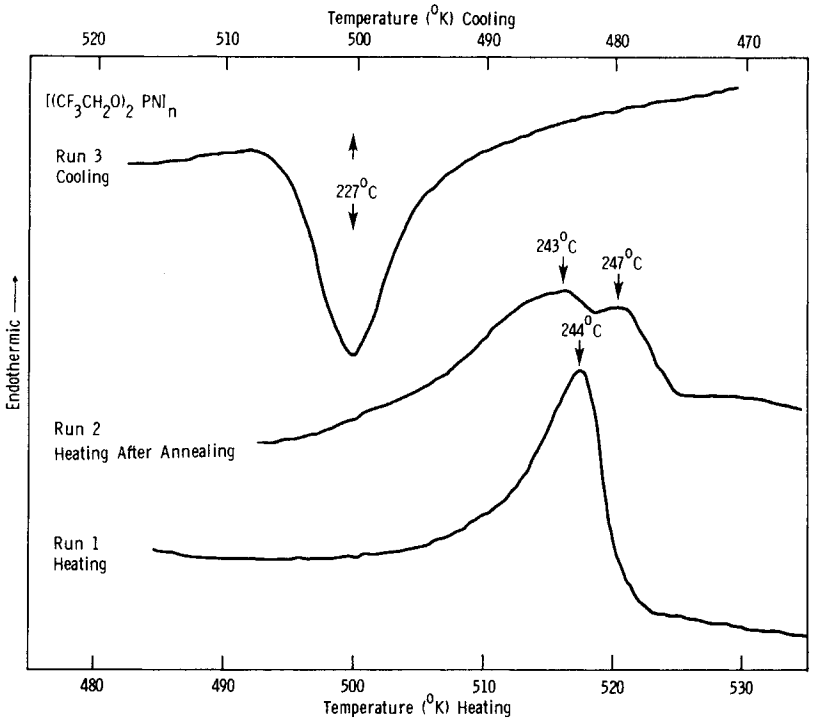

Fig. 7. Expanded melting endotherms and crystallization exotherm at T_m for sample I: runs 1 and 2, heating rate, 10°/min; run 2, after annealing 10 min at 236°C; run 3, cooling rate, 10°/min; attenuation, 0.5 mcal/sec.

The influence of similar thermal treatment on the endotherm at $T(1)$ for sample IIb is shown in Figure 9. The initial endotherm consists of a major low-temperature peak with a high-temperature shoulder. However, in the second run and in run 3, which is merely a repeat at reduced DSC sensitivity, this is replaced by a single sharp endotherm with a peak temperature of 166.5°C. This is higher than the $T(1)$ transition observed in IIa after many cycles, including heating to 525°K. Further cycling of IIb to 450°K or heating to 500°K increases the peak temperature to 168°C, but thereafter the endotherm remains unchanged through a series of additional cycles. Figure 10 shows that the endotherm for IIb not only occurs at higher temperatures than that of IIa but is sharper, with a half-width of 2.5°C compared to 4°C for IIa, and is free of the extensive fraction of low-melting material evident in IIa.

Allen and co-workers[4] have reported a true melting transition for II at temperatures exceeding 350°C observed by optical microscopy and at 405°C by differential thermal analysis (DTA). In a search for T_m, a sample of IIb was scanned at temperatures up to 680°K without revealing any trace of the expected melting peak. Since the scans were made at a sensitivity of 1 mcal/sec and a heating rate of 40°/min, it should be possible to detect an endotherm with about 2% of the enthalpy change at $T(1)$. Although no upper transition was observed, the high-temperature exposure produced some degradation of the sample, as evidenced by a 3°C drop in $T(1)$ and broadening of the peak to a half-width of 5°C.

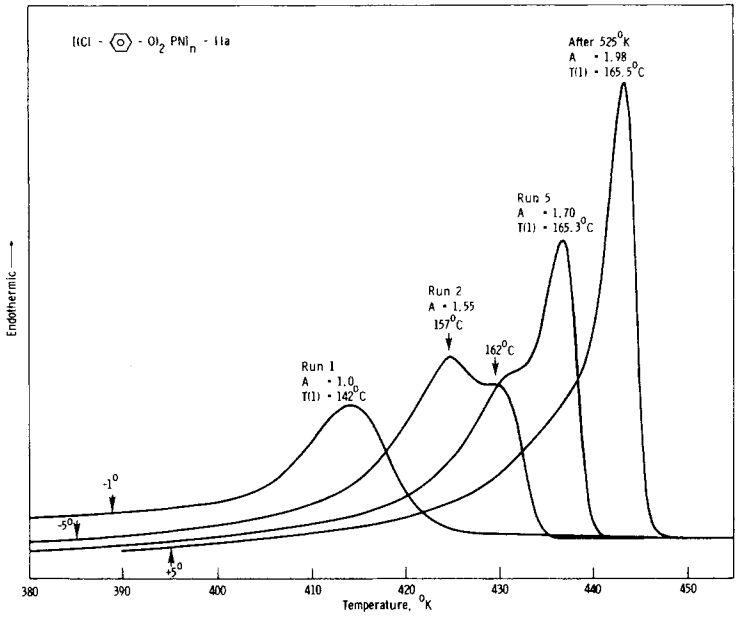

Fig. 8. Influence of thermal cycling on the crystalline-to-mesomorphic transition in IIa: for all runs, heating cycles, 360° to 450°K; heating rate, 10°/min; cooling rate, 40°/min; attenuation, 2 mcal/sec. Curves displaced by amounts indicated near 390°K.

Thermal Mechanical Analysis

The TMA system when used in the penetrometer mode proved to be an effective method for determining the two first-order transitions temperatures in I. With small loadings (5 to 8 g), $T(1)$ appeared as region of expansion, due to the relatively large volume change and comparative rigidity of the sample at this temperature, and T_m as a region of penetration. The transition temperature $T(1)$ taken as the final point of expansion, corresponding to the transformation of the last portion of the crystalline phase, was in good agreement with the DSC results. The value of T_m, interpolated in the usual manner for penetrometer curves, was about 15°C lower than the results from the DSC study. When the penetrometer method was applied to IIb, the lower first-order transition again was clearly defined. However, above $T(1)$, gradual penetration occurred over a broad temperature range preceding the final softening of the sample. The apparent T_m transition determined in successive runs was very sensitive to the probe loading and varied from 240° to 300°C.

Due to the uncertain nature of these results, an examination of the transition behavior was carried out using the TMA system with the thermal expansion probe. Conditions required for reproducible and reliable results were first established with trial runs on I. It was found that, if the sample was cut so that it was smaller than the diameter of the probe, and if the probe was first seated by an initial scan above $T(1)$ with a weight 1 to 5 g greater than the neutral buoyancy point of the probe (about 3 g), it was then possible, after removal of the excess weight, to observe the thermal expansion which occurs both at $T(1)$ and at T_m.

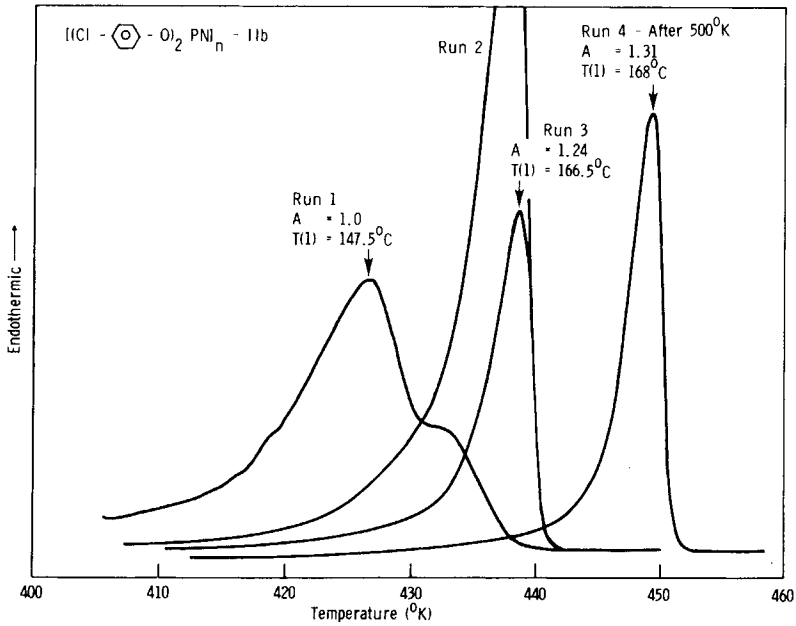

Fig. 9. Influence of thermal cycling on the crystalline-to-mesomorphic transition in IIb: for all runs, heating cycle, 380° to 450°K; heating rate, 10°/min; cooling rate, 40°/min. Runs 1 and 2, attenuation, 2 mcal/sec; run 3, attenuation, 5 mcal/sec; run 4, after heating to 500°K, curve displaced upward 10°.

As shown in Figure 11, the expansion at $T(1)$ is well defined, and almost the full course of the expansion at T_m starting from below 200°C can be observed. Expansion terminates when the sample softens and flows. The value of T_m obtained by this method is about 8°C lower than the temperature determined by DSC. The indicated expansion which occurs at both $T(1)$ and T_m is about 0.5 mil for a sample originally of 12.5-mil thickness, which corresponds to a volume change of about 4% at each transition. The slight change in specimen thickness which occurs when the probe is seated and the flow which occurs as the temperature approaches T_m contribute to uncertainties in the estimate of the percentage volume change. However, such uncertainties do not affect the conclusion that the volume changes at $T(1)$ and T_m are similar in magnitude.

With IIb, a number of exploratory runs showed that well-defined behavior at $T(1)$ was readily obtained but that expansion was replaced by sample flow above 240°C, confirming the existence of a region of decreasing modulus as indicated previously by penetrometer runs. This could be circumvented by further conditioning of the sample. In the run shown in Figure 12, the sample was heated to 300°C under a 5-g load, the load was reduced to 3 g, and the sample was cooled with the probe in place. The upward scan, starting at 230°C in this case and as low as 200°C in other runs, now does not show any evidence of a transition until expansion begins at 330°C which marks the onset of T_m. The interpolated intersection for the transition at 365°C shown in Figure 12 corresponds to an expansion of about 0.74 mil compared to 0.42 mil at $T(1)$ for a 12.5-mil sample. For this polymer, the apparent volume change at T_m is significantly larger than the change at $T(1)$.

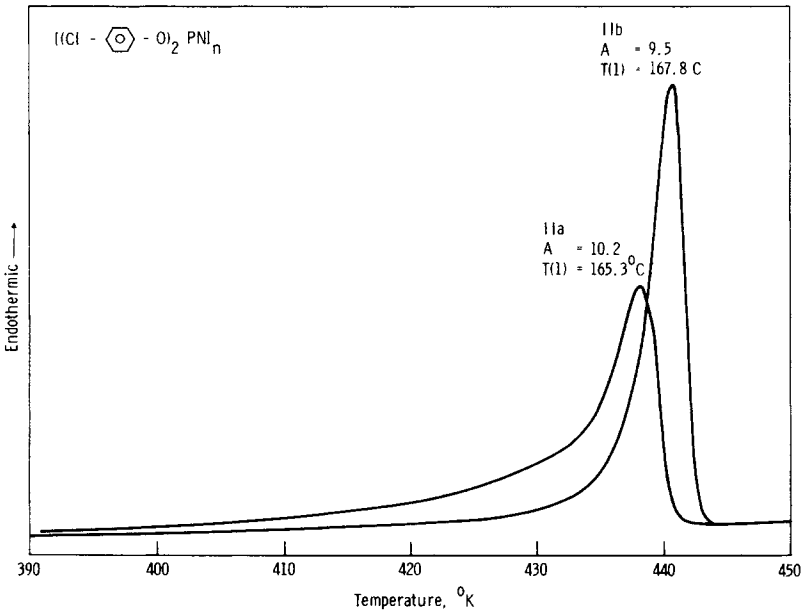

Fig. 10. Comparison of the endotherm at $T(1)$ for samples IIa after heating to 525°K and IIb after heating to 500°K: heating rates, 10°/min; attenuation, 5 mcal/sec.

DISCUSSION AND CONCLUSIONS

The accumulated evidence from the several methods of observation reported by Allen[4] and work presented here indicate that the $T(1)$ transition represents a transformation to a state of partial order in these representative alkoxy- and aryloxy-substituted polyphosphazene samples. Despite the more bulky aryloxy substituent in II, the x-ray diffraction pattern shows two reflections above $T(1)$ with spacings which differ from the single sharp line at 11 Å reported for I by Allen. From the partial orientation existing in the compression-molded sample, it can be concluded that these are very likely hkO lines and therefore indicate lateral chain packing order. A more detailed analysis of the structure of the mesomorphic state for II and the corresponding meta-substituted isomer will be presented in a later paper.[8]

One important conclusion of the results on the thermal transition behavior is the possibility of improving the organization of the mesomorphic state by annealing and, in the case of I, by controlled crystallization from the true melt. This is manifest in the profound influence which the thermal history above $T(1)$ exerts on the characteristics of the crystalline state as indicated both by the improvement in the x-ray diffraction patterns and the increase in the transition temperature, peak area, and sharpness of the endotherm at $T(1)$. Such annealing procedures are important in perfecting the crystalline organization to increase the information which can be obtained from x-ray diffraction studies aimed at solving the structure problem. This was recognized by Bishop and Hall[7] in their work on the unit cell structure of II. However, as with other polymers, the improvement in crystalline organization is bought at the expense of embrittling the sample. In the case of the organo-substituted polyphosphazenes, there is the additional complication that solution-cast films are usually ductile and will

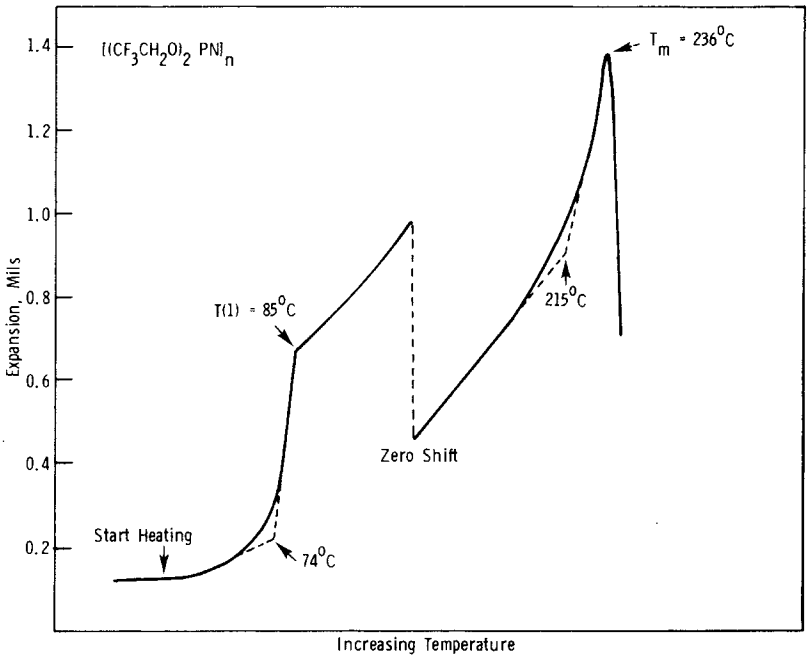

Fig. 11. Thermal expansion curve attained by TMA for sample I: sample thickness, 12.5 mil; heating rate, 20°/min.

undergo cold drawing,[3] whereas compression-molded films including preparations of I and II are brittle. Since a solution-cast film of I after annealing above $T(1)$ becomes brittle, the change must be related to an alteration of the morphology, but the problem is not well understood at this time.

The pronounced differences in the behavior of samples IIa and IIb indicate that there are differences in the structure of these two samples which are otherwise of the same nominal composition as shown in Table I. The conditions used in both steps of the synthesis can affect the structure of the final polymer. It is well known that branching and gelation are favored at higher temperatures and higher conversions in the ring-opening polymerization of the trimer, but other factors which are still not completely defined or controlled can also influence the structure of the polymer prepared in different runs or in different laboratories.[3] As shown in Table I, sample IIb was polymerized for a longer time and at a higher temperature than IIa, but was substituted under more severe conditions.

Some results from solution characterization[9] provide a clue to the nature of the differences in the structure of the two samples. Sample IIa has an intrinsic viscosity in tetrahydrofuran $[\eta] = 3.0$ dl/g and a number-average molecular weight $M_n = 4.4 \times 10^5$ determined by membrane osmometry. Since this sample clogged a 0.45 μ Millipore filter, the weight-average molecular weight could not be determined. For sample IIb, $[\eta] = 1.64$ dl/g (THF), $M_n = 2.2 \times 10^5$, $M_w = 2.1 \times 10^6$, and the sample was readily filterable. Apparently, IIb is lower in molecular weight and free of gel, and presumably has less branching. Work in progress[9] suggests that the more severe substitution conditions used for IIb are capable of reducing the molecular weight and extent of branching by chain scission which

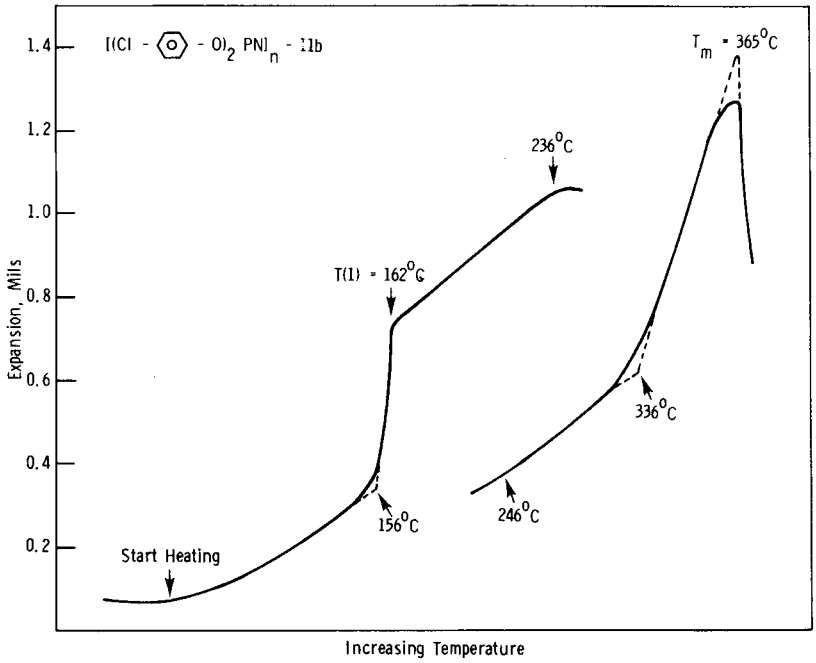

Fig. 12. Thermal expansion curve attained by TMA for sample IIb: sample thickness, 12.5 mil; heating rate, 20°/min.

occurs preferentially at branch points. The site of other chain defects such as incompletely substituted phosphorus chain atoms may be similarly affected by the more severe substitution conditions used in the preparation of IIb, with the result that IIb is a cleaner sample than IIa. Probably some of the change in the endotherm of IIa on thermal cycling is due to thermally induced chain scission at such branch points and impurity locations in the polymer chain.

There are further complications in the thermal transition behavior due to the possibility of some depolymerization to cyclic organophosphazenes at elevated temperatures.[10,11] In addition, experiments which will be described in detail elsewhere[12] indicate that the small amount of cyclic and oligomeric species present in these samples facilitate the improvement in crystalline order which is brought about by thermal cycling. However, this observation does not alter the conclusion that the differences in the responses of IIa and IIb to thermal treatment are due primarily to differences in branching and other chain defects.

A summary of the thermal transition data of the two polyphosphazenes in a comparison with other samples is presented in Table II. The enthalpy change at $T(1)$ is far smaller than the values generally observed for the melting of polymers, even by comparison with polyacrylonitrile which contains only two-dimensional crystallinity.[13] The small enthalpy change is probably characteristic of the transition from a crystalline to partially ordered state and the large temperature range between $T(1)$ and T_m, although allowance must be made for the presence of a small fraction of amorphous material. Of equal significance are the very low values of ΔH at T_m which indicate that there is very little difference in the intermolecular interactions which occur in the partially ordered state and the melt. Therefore, it is surprising to find that the estimated volume changes

at the two transitions are of the same magnitude. The most nearly analogous behavior to ΔH and ΔV is observed in certain liquid crystals as indicated by the results in Table III for *p*-azoxyanisole.[14]

The appearance of mesomorphic structure in polymers is the subject of increasing attention. One of the questions which need to be answered in making useful comparisons with this published work is whether the mesomorphic state in certain polyphosphazenes is determined by the nature of the substituents or is characteristic of the backbone structure. The results which have recently been tabulated indicating that the mesomorphic state occurs in polyphosphazenes with a wide variety of substituent composition[3] suggest that the second alternative applies, and further evidence supporting this conclusion will be published shortly. Therefore, comparisons can be limited to polymers where the occurrence of the state of intermediate order is related to the backbone structure.

Polyacrylonitrile is one of the more prominent examples where the atactic nature of the chain structure prohibits three-dimensional crystallinity but where two-dimensional crystallinity involving ordered packing of the chains occurs.[13] This partially ordered state is made possible by the small van der Waals radius of the nitrile group. In the model advanced for II by Bishop and Hall, there is very little interpenetration of the side groups, and the chain packing is determined largely by the outer cylinderical envelope. In this sense, there may be a relation between the packing in polyacrylonitrile and the mesomorphic state for certain polyphosphazenes. However, there is also a fundamental difference between the two in that polyacrylonitrile lacks the fluidity characteristic of the liquid crystal state and of polyphosphazenes above the $T(1)$ transition.

Poly(oxybenzoyl)

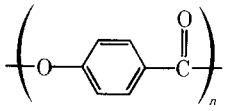

undergoes a transition at 340° to 360°C to a one-dimensional crystal in which only the registry of atoms along the chain direction is maintained.[15,16] Since the polymer decomposes below the melting temperature of 550°C, it is formed by sintering or forging above the crystal–crystal transition where the reduction in interchain forces facilitates shearing of the crystals. The material, however, is still very rigid in this temperature interval. The rigidity and symmetry of the chain and nature of the mesomorphic state in this case appear very different from the characteristics of the polyphosphazenes.

More recently, a series of polymers containing benzalazine as part of the repeat unit

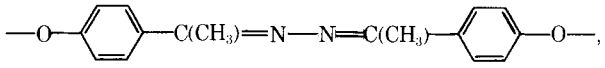

which is similar to certain low molecular weight liquid crystals, have been reported to display $T(1)$ and T_m transition separated by about 50°C.[17] This class of materials appears to bear little structural relation to the polyphosphazenes, which are flexible and lack the semirigid and highly asymmetric structure units of the benzalazine polymers. The existence of a mesomorphic transition in poly(diethylsiloxane), $[(C_2H_5)_2\ SiO]_n$, has been reported by Beatty and coworkers.[18] The polyphosphazenes resemble the siloxanes in terms of flexibility

and certain features of backbone structure.[3] But the mesomorphic state in poly(diethylsiloxane), which has been termed a viscous crystalline state, is limited to a range of 25° between $T(1)$ and T_m.

Thus, while certain analogies exist with the mesomorphic state which occurs in other polymers, the occurrence of a crystalline-to-mesomorphic state which is stable over a temperature range as great at 300°C is unusual and depends on special features of the polyphosphazenes structure which at present are not clearly identified. Studies are continuing in order to characterize the structure of the mesomorphic state and additional features of the transition behavior for the poly(organophosphazenes) reported on here. Work is also in progress on a number of other aryloxy polyphosphazenes with varied substituent structure.

References

1. H. R. Allcock and R. J. Kugel, *J. Amer. Chem. Soc.*, **87,** 4216 (1965).
2. H. R. Allcock, *Chem. Rev.*, **72,** 315 (1972).
3. R. E. Singler, N. S. Schneider, and G. L. Hagnauer, *Polym. Sci. Eng.*, **15,** 322 (1975).
4. G. Allen, C. J. Lewis, and S. M. Todd, *Polymer*, **11,** 44 (1970).
5. T. M. Connelly and J. K. Gilham, *J. Appl. Polym. Sci.*, **20,** 473 (1976).
6. K. A. Reynard, A. H. Gerber, and S. H. Rose, *Synthesis of Phosphonitrile Elastomers and Plastics for Marine Applications*, AMMRC CTR 72-29, Dec. 1972 (AD 155188).
7. S. M. Bishop and I. H. Hall, *Brit. Polym. J.*, **6,** 193 (1974).
8. C. R. Desper and N. S. Schneider, *Macromolecules*, in press.
9. G. L. Hagnauer, B. R. LaLiberte, and R. E. Singler, U.S. Army Materials & Mechanics Research Center, unpublished work, (1974–1975).
10. H. R. Allcock and W. J. Cook, *Macromolecules*, **1,** 284 (1974).
11. H. R. Allcock, G. Y. Moore, and W. J. Cook, *Macromolecules*, **1,** 571 (1974).
12. J. Beres, U.S. Army Materials & Mechanics Research Center, unpublished work, 1975.
13. C. R. Bohn, J. R. Schaefgen, and W. O. Statton, *J. Polym. Sci.*, **55,** 531 (1961).
14. D. B. Du Pre, E. T. Samulski, and A. V. Tobolsky, in *Polymer Science and Materials*, A. V. Tobolsky and H. F. Mark, Eds., Wiley-Interscience, New York, 1971, Chap. 7.
15. S. G. Cottis and J. Economy, in *Condensation Monomers*, Vol. 27 of *High Polymers*, J. K. Stille, Ed., Wiley-Interscience, New York, 1972, Chap. 3.
16. S. G. Cottis, The Carborundum Company, personal communication, 1975.
17. A. Roviello and A. Sirigu, *J. Polym. Sci., Polym. Lett. Ed.*, **13,** 455 (1975).
18. C. L. Beatty, T. M. Pochan, M. F. Froix, and D. D. Hinman, *Macromolecules*, **8,** 547 (1975).

Received October 17, 1975
Revised December 22, 1975